Precision Measurement of $\pi\pi$ Scattering Lengths in K_{e4} Decays

D. T. Madigozhin[a*] on behalf of the NA48/2 Collaboration
[a] *Joint Institute for Nuclear Research*
Russia, 141980 Moscow region, Dubna, Joliot-Curie 6, JINR

Abstract

The measurement of the S-wave $\pi\pi$ scattering lengths is a fundamental test of the validity of Chiral Perturbation Theory. We report on the final NA48/2 result, which uses the complete NA48/2 data set with more than one million reconstructed $K^{\pm}_{e4}$ decays. From these events we have determined the decay form factors and $\pi\pi$ scattering lengths a_0^0 and a_0^2. The result is the currently most precise measurement of the scattering lengths and in excellent agreement with the prediction of Chiral Perturbation Theory.

1 Introduction

Chiral Perturbation Theory (ChPT) is very powerful in describing $\pi\pi$ at low energy. The underlying constants of the theory, a_0^0 and a_0^2, are the S-wave pion-pion scattering lengths in the isospin 0 and 2 states.

The study of K_{e4} is of particular interest as it is explores the two-pion final state interaction in the absence of any other hadron. Under the assumption of isospin symmetry, the measurement of a_0^0 and a_0^2, based on a partial sample collected in 2003, has been reported by NA48/2 collaboration at the CERN SPS [1].

Recently, precise experimental measurements of these scattering lengths have been also performed by NA48/2 in the study of $K^{\pm} \to \pi^{\pm}\pi^0\pi^0$ decays [2, 3]. It has shown the first evidence for a cusp-like structure in the $\pi^0\pi^0$ invariant mass distribution, explained by $\pi\pi$ scattering effects near the $2m_{\pi^{\pm}}$ threshold. Another approach is the formation of the $\pi\pi$ atoms, as studied by the DIRAC collaboration [4].

The final results from the NA48/2 K_{e4} full statistics analysis (1.13 million decays), taking into account isospin symmetry breaking effects, are reported here. A measurement of a_0^0 and a_0^2, based on the combined K_{e4} and cusp results, will also be given.

2 Beam and detectors

Two simultaneous K^+ and K^- beams are produced by 400 GeV/c protons impinging on a beryllium target. Particles of opposite charge with a central momentum of 60 GeV/c and a momentum band of $\pm 3.8\%$ (rms) are selected by two systems of dipole magnets, focusing quadrupoles, muon sweepers and collimators. The decay volume is a 114 m long vacuum space.

A detailed description of the detector elements is available in [5]. Charged particles from $K^{\pm}$ decays are measured by a magnetic spectrometer consisting of four drift chambers (DCH1–DCH4) and a dipole magnet located between DCH2 and DCH3. Each chamber has eight planes of sense wires, two horizontal, two vertical and two along each of two orthogonal 45° directions. The spectrometer is located in a tank filled with helium at atmospheric pressure and separated

*e-mail: madigo@mail.cern.ch

from the decay volume by a thin $Kevlar^{\textcircled{R}}$ window. A 16 cm diameter aluminum vacuum tube centred on the beam axis runs the length of the spectrometer through central holes in the window, drift chambers and calorimeters. Charged particles are magnetically deflected in the horizontal plane by an angle corresponding to a transverse momentum kick of 120 MeV/c. The momentum resolution of the spectrometer is $\sigma(p)/p = 1.02\% \oplus 0.044\%p$ (p in GeV/c). The magnetic spectrometer is followed by a scintillator hodoscope.

A liquid Krypton calorimeter (LKr) [6] is used to measure the energy of electrons and photons. It is an almost homogeneous ionization chamber with an active volume of ~ 10 m^3 of liquid krypton, segmented transversally into 13248 2 cm $\times$ 2 cm projective cells by a system of Cu-Be ribbon electrodes. The calorimeter is 27 X_0 thick and has an energy resolution $\sigma(E)/E = 0.032/\sqrt{E} \oplus 0.09/E \oplus 0.0042$ (E in GeV). The space resolution for single electromagnetic showers can be parameterized as $\sigma_x = \sigma_y = 0.42/\sqrt{E} \oplus 0.06$ cm for each transverse coordinate x, y.

3 Event selection and background rejection

The data sample was selected for three reconstructed charged tracks in time with the corresponding hodoscope signals. The three-track reconstructed vertex was required to lie within a 5 cm radius transverse to the beam axis. Two opposite sign pions ($E/p < 0.8$) and one electron or positron ($0.9 < E/p < 1.1$) were required. The minimum momenta of pion (electron) were 5 GeV/c (3 GeV/c), while the maximum momentum sum was set at 70 GeV/c.

The distance between any two tracks at DCH1 was required to be larger than 2 cm, and the distance between any track and the beam axis larger than 12 cm.

Fiducial cuts on the distance of each track impact at the LKr front face from the LKr edges and centre were also applied in order to ensure full containment of the electromagnetic showers. The minimum distance between the track impact at the LKr front face and the nearest LKr dead cell was required to be at least 2 cm. The track-to track distance at the LKr front face had to be larger than 20 cm to prevent shower overlaps.

The reconstruction of the kaon momentum assuming a four-body decay with the undetected neutrino was implemented, and the solution closer to 60 GeV/c was assigned to p_K. Events with kaon momentum between 54 and 66 GeV/c were kept for further analysis.

There are two main background sources: $K^\pm \to \pi^+\pi^-\pi^\pm$ decays with subsequent $\pi \to e\nu$ decay or a pion mis-identified as an electron; and $K^\pm \to \pi^0(\pi^0)\pi^\pm$ with subsequent $\pi^0 \to e^+e^-\gamma$ decay with undetected photons and an electron mis-identified as a pion.

Events with hard photon emission were rejected to avoid biasing kinematic reconstruction. Cuts on three-track invariant mass and transverse momentum were also applied to reject background. A dedicated linear discriminant variable (LDA) based on shower properties has been developed to reject events with one misidentified pion.

The background contamination was estimated from the "wrong sign" events (two same sign pions), which can only be background. To estimate the "right sign" part of the background in the selected sample, the number of "wrong sign" events has to be multiplied by 2, as the dominant contribution comes from $K^\pm \to \pi^+\pi^-\pi^\pm$ decays and is confirmed by Monte Carlo simulation studies. The 0.6% background contribution was found to be constant during the data taking period.

4 K_{e4}: theoretical formulation

The kinematics of the $K^\pm \to \pi^+\pi^- e^\pm \nu$ decay is described by the five Cabibbo-Maksymowicz variables [7]: the square of the dipion invariant mass S_π, the square of the dilepton invariant mass S_e, the angle θ_π of the $\pi^\pm$ in the dipion rest frame with respect to the flight direction of the dipion in the kaon rest frame, the angle θ_e of the $e^\pm$ in the dilepton rest frame with respect

to the flight direction of the dilepton in the kaon rest frame, and the angle ϕ between the dipion and dilepton planes in the kaon rest frame.

The decay amplitude is the product of the leptonic weak current and the (V-A) hadronic current:

$$\frac{G_w}{\sqrt{2}} V_{us}^* \bar{u}_\nu \gamma_\lambda (1-\gamma_5) v_e (< \pi^+\pi^- | V^\lambda | K^+ > - < \pi^+\pi^- | A^\lambda | K^+ >). \quad (1)$$

The hadronic current is described by three (F,G,R) axial-vector and one (H) vector complex form factors.

These form-factors may be developed in a partial wave expansion with respect to the variable $cos\theta_\pi$:

$$\begin{aligned} F &= F_s e^{i\delta_{fs}} + F_p e^{i\delta_{fp}} cos\theta_\pi + F_d e^{i\delta_{fd}} cos^2\theta_\pi + ... \\ G &= G_p e^{i\delta_{gp}} + G_d e^{i\delta_{gd}} cos\theta_\pi + ... \\ H &= H_p e^{i\delta_{hp}} + H_d e^{i\delta_{hd}} cos\theta_\pi + ... \end{aligned} \quad (2)$$

Limiting the expansion to S- and P-waves and considering a unique phase δ_p for all P-wave form factors in absence of CP violating weak phases, the decay probability depends only on the form factor magnitudes F_s, F_p, G_p, H_p, a single phase $\delta = \delta_s - \delta_p$ and kinematic variables.

5 Analysis

To take into account the precise knowledge of experimental acceptance and resolution, we define a grid of equal population boxes in the five-dimensional space. The data sample is first distributed over ten $M_{\pi\pi}$ slices to follow the variation of physical parameters along this variable; each sub-sample is then distributed over five $M_{e\nu}$ slices, then over five $cos\theta_\pi$ slices, five $cos\theta_e$ slices and twelve ϕ slices.

A detailed GEANT3-based [8] Monte Carlo simulation was used to take into account full detector geometry, DCH alignment, local inefficiencies and beam properties. The quality of the simulation can be seen from the comparison of simulated and data distributions (Figures 1).

A Log-likelihood dedicated estimator is used to minimize the difference between the measured numbers of data and expected simulated events in the each box. The fit results are found consistent for both kaon charge signs and then combined in each $M_{\pi\pi}$ bin according to their statistical weight. A comparison of data and simulated distributions after fit is shown in Figure 2 for some of the Cabibbo-Maksymowicz variables.

In a second stage of the analysis, the observed variations of the form factors with energy are used to determine other parameters values through specific models. Under the assumption of isospin symmetry, the form factors can be developed in a series expansion of the dimensionless invariants $q^2 = (S_\pi/4m_\pi^2) - 1$ and $S_e/4m_\pi^2$ [9].

Two slope and one curvature terms are sufficient to describe the measured F_s form factor variation within the available statistics ($F_s = f_s(1 + f_s'/f_s q^2 + f_s''/f_s q^4 + f_e'/f_s S_e/4m_\pi^2)$), while two terms are enough to describe the G_p form factor ($G_p/f_s = g_p/f_s + g_p'/f_s q^2$), and two constants to describe the F_p and H_p form factors:

$$\begin{aligned} f_s'/f_s &= \quad 0.152 \pm 0.007_{stat} \pm 0.005_{syst} \\ f_s''/f_s &= -0.073 \pm 0.007_{stat} \pm 0.006_{syst} \\ f_e'/f_s &= \quad 0.068 \pm 0.006_{stat} \pm 0.007_{syst} \\ f_p/f_s &= -0.048 \pm 0.003_{stat} \pm 0.004_{syst} \\ g_p/f_s &= \quad 0.868 \pm 0.010_{stat} \pm 0.010_{syst} \\ g_p'/f_s &= \quad 0.089 \pm 0.017_{stat} \pm 0.013_{syst} \\ h_p/f_s &= -0.398 \pm 0.015_{stat} \pm 0.008_{syst} \end{aligned}$$

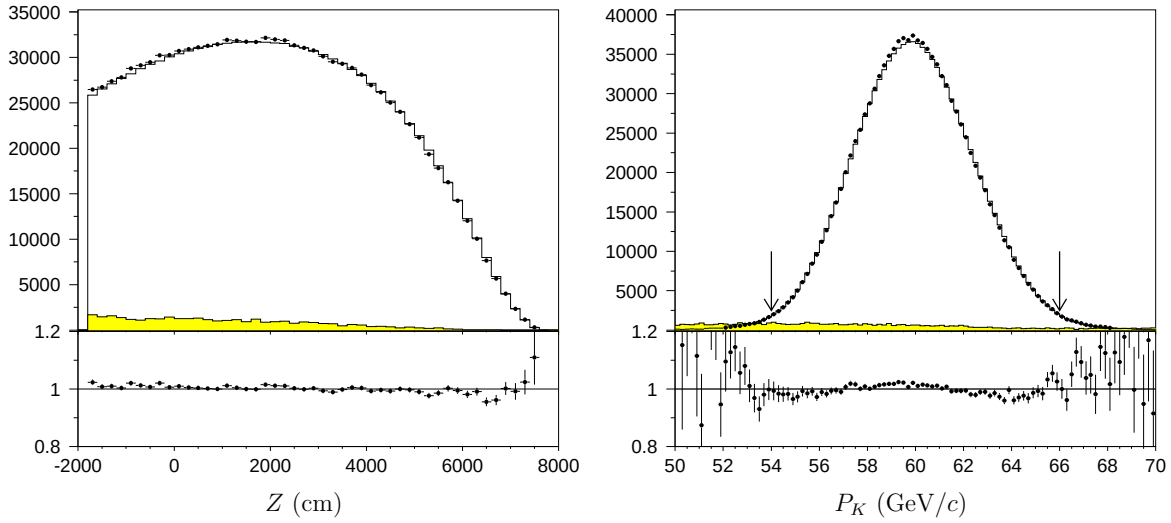

Figure 1: Distributions of the reconstructed vertex longitudinal position Z (left) and the reconstructed kaon momentum P_K (right). Data (background subtracted) are shown as full circles with error bars, simulations as histograms and background (wrong sign events increased by a factor of 10 to be visible) as shaded areas. The inserts show the ratio of data to simulated distributions. The arrows on the right plot show the reconstructed kaon momentum range selected in the final analysis.

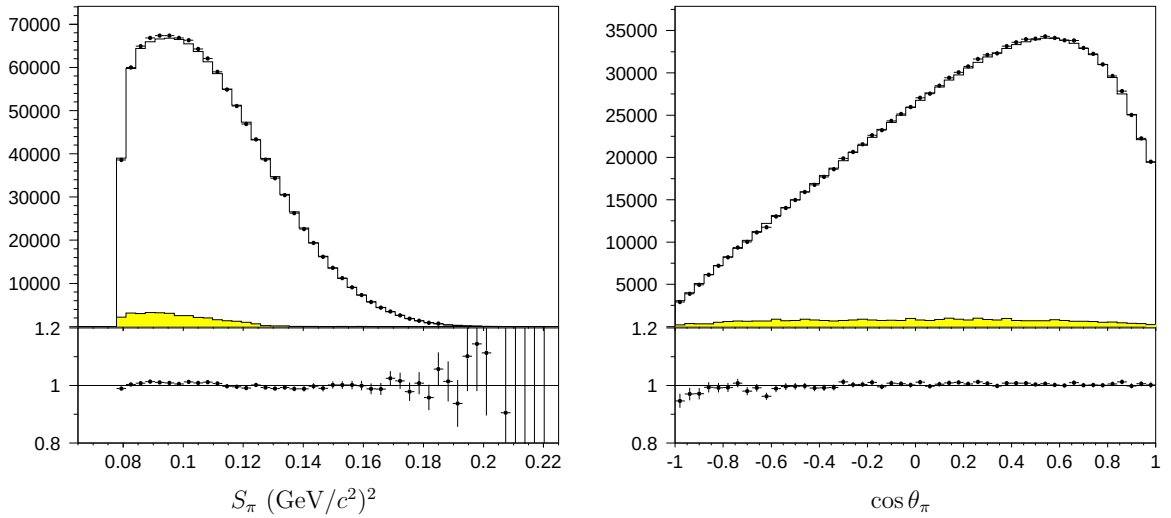

Figure 2: Distribution of two Cabibbo-Maksymowicz variables projected from the five-dimensional space. Notation is the same as in Figure 1.

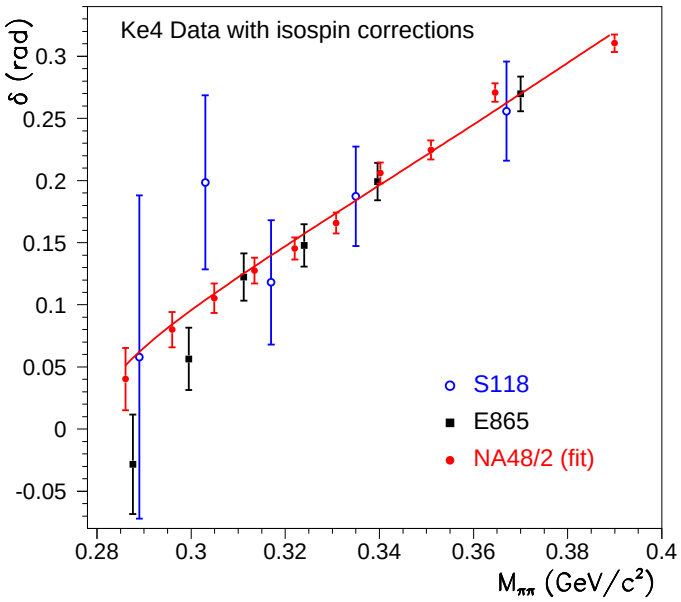

Figure 3: Phase shift (δ) measurements corrected for isospin mass effects for all K_{e4} available results ([13, 14, 15]). The line corresponds to the two-parameter fit of the NA48/2 data alone.

6 Results of $\pi\pi$ scattering lengths measurement

Roy equations [10] are based on the fundamental principles of analyticity, unitarity and crossing symmetries, and allow a calculation of the phase shift δ using experimental measurements at $\sqrt{s} > 0.8$ GeV and the subtraction constants a_0^0 and a_0^2, the S-wave scattering lengths for the isospin 0 and 2 (we will express them here in units of $m_{\pi^+}^{-1}$). To extract these lengths we use the Roy equations numerical solution polynomial parameterisation [11]. The a_0^0 and a_0^2 values are constrained to lie within a "Universal Band", fixed by the input data above 0.8 GeV and the Roy equations.

Recent theoretical work [12], triggered by NA48/2 measurements, has shown, that isospin symmetry breaking effects also alter the measured phases if mass difference between charged and neutral pion and between u and d quarks are considered. The change is modest in terms of absolute magnitude (10 – 15 mrad), but the coherent increase of the phase values leads to a shift of the measured $\pi\pi$ scattering lengths, and is quite essential when the precision of NA48/2 final results is reached.

These theoretical ingredients have been used to extract a_0^0 and a_0^2 values from the NA48/2 K_{e4} data.

For the two-parameter fit (with a_0^0 and a_0^2 as free parameters), the following result has been obtained:

$$\begin{aligned} a_0^0 &= 0.2220 \pm 0.0128_{stat} \pm 0.0050_{syst} \pm 0.0037_{th}; \\ a_0^2 &= -0.0432 \pm 0.0086_{stat} \pm 0.0034_{syst} \pm 0.0028_{th}. \end{aligned} \tag{3}$$

with a 97% correlation coefficient. These values test ChPT predictions, as we do not use ChPT ingredients to extract them.

In the framework of ChPT, an additional constraint could be used [16] to obtain a measurement with reduced errors:

$$a_0^2 = (-0.0444 \pm 0.0008) + 0.236(a_0^0 - 0.22) - 0.61(a_0^0 - 0.22)^2 - 9.9(a_0^0 - 0.22)^3 \tag{4}$$

Using this additional ChPT constraint (Eq(4)), the one-parameter fit gives:

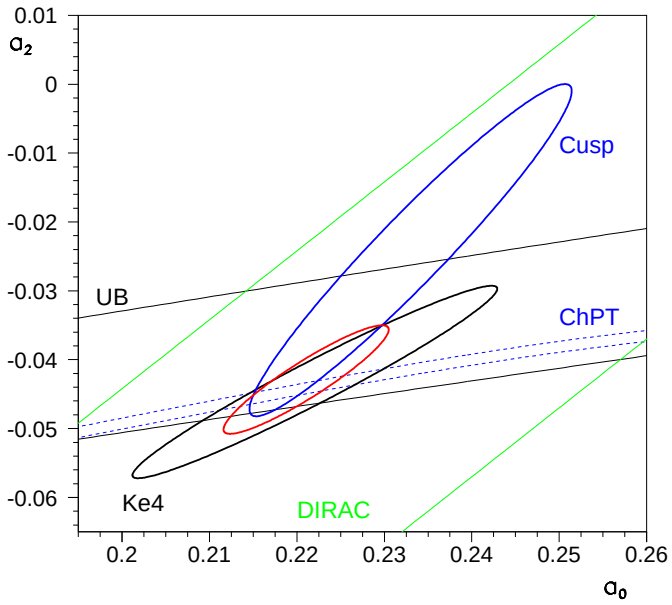

Figure 4: NA48/2 Ke4 and cusp results from the two-parameter fits, 68% confidence level ellipses are shown. The smallest contour corresponds to combination of the two NA48/2 results. The dashed lines visualize the ChPT constraint band and the solid lines the Universal Band (UB). The other lines correspond to the DIRAC result band [4].

$$a_0^0 = 0.2206 \pm 0.0049_{stat} \pm 0.0018_{syst} \pm 0.0064_{th}. \tag{5}$$

Systematical errors include contributions from sensitivity to the fit procedure, trigger efficiency, muon veto inefficiency, acceptance and resolution simulation quality, background shape and overall level, electron identification, radiative corrections control and neglected form factors S_e dependence.

The theoretical errors are dominated by the experimental precision of the inputs to the Roy equation and the neglected higher order terms in the mass effects calculation.

Figure 4 compares our results with the results from the cusp effect final analysis in the $K^\pm \to \pi^\pm\pi^0\pi^0$ decay, also performed by the NA48/2 collaboration [2, 3]. The cusp and K_{e4} results are statistically independent and have systematic uncertainties of different nature. Moreover, the two results show different correlations between the fitted scattering lengths and can be combined to obtain an improved precision.

Neglecting theoretical uncertainties and small common systematic contribution to the experimental errors, the combination of the two measurements is ($\chi^2/ndf = 1.84/2$):

$$\begin{aligned} a_0^0 &= 0.2210 \pm 0.0047_{stat} \pm 0.0040_{syst}, \\ a_0^2 &= -0.0429 \pm 0.0044_{stat} \pm 0.0028_{syst}, \end{aligned} \tag{6}$$

with a 92% correlation coefficient (small ellipse on Figure 4).

When using the ChPT constraint, the combined NA48/2 results become ($\chi^2/ndf = 1.87/1$):

$$\begin{aligned} a_0^0 &= 0.2196 \pm 0.0028_{stat} \pm 0.0020_{syst}, \\ a_0^2 &= -0.0444 \pm 0.0007_{stat} \pm 0.0005_{syst} \pm 0.0008_{ChPT}, \end{aligned} \tag{7}$$

where the $ChPT$ error comes from the ChPT constraint uncertainty.

From the measurement of the pionium lifetime by the DIRAC experiment at the CERN PS [4] a value of $|a_0^0 - a_0^2| = 0.264^{+0.033}_{-0.020}$ was deduced which agrees, within its quoted uncertainty, with our result.

Both K_{e4} alone and combined NA48/2 results are in a good agreement with theoretical calculations performed in the framework of Chiral Perturbation Theory [17, 18], which predict ($a_0^0 = 0.220 \pm 0.005$ and $a_0^2 = -0.0.0444 \pm 0.0010$.

Conclusion

The analysis of 1.13 millions K_{e4} decays has been performed by the NA48/2 collaboration. Form factors of the decay matrix element are measured with the currently best available precision.

The precise measurement of the $\pi\pi$ system phase shift in K_{e4} decays has allowed to extract the scattering lengths a_0^0 and a_0^2, using Roy equation and taking into account isospin symmetry breaking effects.

Our results agree with the values of the $\pi\pi$ scattering lengths obtained from the study of the cusp effect. Both NA48/2 results have been combined to obtain even more precise scattering lengths values. This very stringent test strongly confirms the predictions of Chiral Perturbative Theory and its underlying assumptions.

References

[1] J. Batley et al. (NA48/2), Eur. Phys. J. **C54** (2008) 411.

[2] J.R. Batley et al. (NA48/2), Phys. Lett. **B633**, 173 (2006), `hep-ex/0511056`

[3] J. Batley et al. (NA48/2), Eur. Phys. J. **C64** (2009) 589.

[4] B. Adeva et al. (DIRAC), Phys. Lett. **B619**, 50 (2005), `hep-ex/0504044`

[5] V. Fanti et al. (NA48), Nucl. Instrum. Meth. **A574**, 433 (2007)

[6] G.D. Barr et al. (NA48), Nucl. Instrum. Meth. **A370**, 413 (1996)

[7] N. Cabibbo and A. Maksymowicz, Phys. Rev. **137** (1965) B438; Phys. Rev. **168** (1968) 1926.

[8] GEANT Description and Simulation Tool, CERN Program Library Long Writeup W5013 (1994).

[9] G. Amoros and J.Bijnens, J. Phys. **G25** (1999) 1607.

[10] S. Roy, Phys. Lett. **B36** (1971) 353.

[11] B. Ananthanarayan, G. Colangelo, J. Gasser, H. Leutwyler, Phys. Rep. **353** (2001) 207.

[12] G. Colangelo, J. Gasser and A. Rusetsky, Eur. Phys. J. **C59** (2009) 777.

[13] L. Rosselet et al. (S118), Phys. Rev. **D15** (1977) 574.

[14] S. Pislak et al. (E865), Phys. Rev. Lett. **87** (2001) 221801; ibid. **105** (2010) 019901.

[15] S. Pislak et al. (E865), Phys. Rev. **D67** (2003) 072004; ibid. **D81** (2010) 119903(E).

[16] G. Colangelo, J. Gasser, H. Leutwyler, Phys. Rev. Lett. **86**, 5008 (2001), `hep-ph/0103063`

[17] G. Colangelo, J. Gasser, H. Leutwyler, Phys. Lett. **B488**, 261 (2000), `hep-ph/0007112`

[18] G. Colangelo, J. Gasser, H. Leutwyler, Nucl. Phys. **B603**, 125 (2001), `hep-ph/0103088`